

# Towards a global network of gamma-ray detector calibration facilities

Marco Tijs<sup>1</sup> Ronald Koomans<sup>1</sup> Han Limburg<sup>1,2</sup>

<sup>1</sup>Medusa Sensing BV, Verlengde Bremenweg 4, 9723JV Groningen, The Netherlands.

<sup>2</sup>Corresponding author. Email: [han@medusa-online.com](mailto:han@medusa-online.com)

**Abstract.** Gamma-ray logging tools are applied worldwide. At various locations, calibration facilities are used to calibrate these gamma-ray logging systems. Several attempts have been made to cross-correlate well known calibration pits, but this cross-correlation does not include calibration facilities in Europe or private company calibration facilities.

Our aim is to set-up a framework that gives the possibility to interlink all calibration facilities worldwide by using ‘tools of opportunity’ – tools that have been calibrated in different calibration facilities, whether this usage was on a coordinated basis or by coincidence.

To compare the measurement of different tools, it is important to understand the behaviour of the tools in the different calibration pits. Borehole properties, such as diameter, fluid, casing and probe diameter strongly influence the outcome of gamma-ray borehole logging. Logs need to be properly calibrated and compensated for these borehole properties in order to obtain in-situ grades or to do cross-hole correlation. Some tool providers provide tool-specific correction curves for this purpose. Others rely on reference measurements against sources of known radionuclide concentration and geometry.

In this article, we present an attempt to set-up a framework for transferring ‘local’ calibrations to be applied ‘globally’. This framework includes corrections for any geometry and detector size to give absolute concentrations of radionuclides from borehole measurements. This model is used to compare measurements in the calibration pits of Grand Junction, located in the USA; Adelaide (previously known as AMDEL), located in Adelaide Australia; and Stonehenge, located at Medusa Explorations BV in the Netherlands.

**Key words:** calibration, gamma ray, logging, MCNP, model pits, uranium.

Received 8 February 2016, accepted 11 August 2016, published online 22 September 2016

## Introduction

In borehole mapping, the concentration of natural radionuclides is an important variable for well-log interpretation. As a result, gamma-ray logging tools are applied worldwide. To get a quantified measurement of the activity concentrations, a probe needs to be calibrated carefully. Typically, this is done by placing the probe in pit with well known activity concentrations and geometry. To compare the measurements of different tools, it is important to understand the behaviour of the tools in the different calibration pits. These calibration pits are distributed all over the world and several attempts have been made to cross-correlate well known ones, but this cross-correlation does not include calibration facilities in Europe or private company calibration facilities. Our aim is to set-up a framework that gives the possibility to interlink all calibration facilities worldwide by using ‘tools of opportunity’ – tools that have been calibrated in different calibration facilities, whether this usage was on a coordinated basis or by coincidence.

A comparison of various tools in various pits is not straightforward. Various types of scintillator-based spectral gamma probes are being used nowadays to measure <sup>40</sup>K, <sup>238</sup>U and <sup>232</sup>Th concentrations in boreholes. This evidently yields a tool ready for use in boreholes of similar geometry. However, for borehole environments that do not match the calibration borehole, the measured nuclide activity concentrations need to be corrected (Bristow et al., 1982).

Chartbooks include correction factors for variations in borehole diameter, fluid density and casing thickness (Schlumberger, 2009;

Weatherford, 2006). However, these have been determined by experiment for borehole probes with two different diameters. As a result, these charts are only useable for a limited number of situations.

Maučec et al. (2009) provide correction formulae based on a large set of Monte Carlo nuclear particle (MCNP) simulations, but due to limited computer resources at that time, the authors were forced to restrict their simulations to a relatively small set of parameters while only changing one borehole parameter at a time.

van der Graaf et al. (2011) explain how to translate the calibration of a scintillation detector from one environment to another environment by comparing the results from Monte Carlo simulations for both environments. The same method can also be applied for a whole range of different environments.

The article we present here, summarises over 500 full spectrum simulations that we have run using the MCNPX code (Waters et al., 2007) in an effort to better understand the various parameters involved in borehole logging. Dickson and Beckitt (2013) have performed a similar study for total count logging tools using the GEANT code.

In our study, we have included the following parameters and ranges in the simulations:

- Probe diameter from 0.5 to 3.4 inch;
- Borehole diameter from 1 to 12 inch;
- Casing thickness up to 25 mm steel or 100 mm PVC;
- Formation density from 1 to 2.65 kg/L; and
- Borehole filled with air or 1 to 2 kg/L bentonite ‘mud’.

All simulations ran for at least 3 h on a desktop computer and produced a spectrum for each of the three radio nuclides ( $^{40}\text{K}$ ,  $^{238}\text{U}$  and  $^{232}\text{Th}$ ) between 0 and 3 MeV in bins of 10 keV.

In most cases, changing one of the borehole parameters has an almost linear effect over all the energy bins above 300 keV. Therefore, in most cases we summarise the data by taking the sum of the bins above 300 keV into the comparison.

In this paper, we describe the effects of the corrections needed to cross-correlate the calibration pits of Stonehenge, Grand Junction (Stromswold, 1995) and Adelaide (Dickson, 2012) for several  $1 \times 4$  inch Bismuth Germanate gamma spectrometers. This approach will provide a framework of cross-correlating other spectral gamma tools.

### Effects of formation density

Maučec et al. (2009) found that the formation density had a significant effect on the count rate, where an increase in the density would result in an increasing probability for a gamma particle to be registered by the detector. Hendriks et al. (2001) attributes this to a combination of the change in geometry and the effects of changing water content.

To verify these results, a series of Monte Carlo models were run assuming a cylindrical BGO detector  $50 \times 150$  mm, located in an ‘infinite’ (1 m radius) source. The borehole in the model has a diameter of 70 mm and is filled with water. The borehole and the probe are identical to the model used by Maučec et al. (2009). The formation is modelled with various densities, either as pure  $\text{SiO}_2$ , or a mixture of  $\text{SiO}_2$  and water. For the latter set, the  $\text{SiO}_2$  is considered to have a density 2.65 kg/L, and water 1.00 kg/L. The ratio between  $\text{SiO}_2$  and water is enough to obtain the desired average density. Results for both sets are shown in Figure 1.

Contrary to the results from the simulations by Maučec et al. (2009), we only found a limited decrease in the count rate for decreasing formation densities for the ‘dry’ situation (pore space empty) (see solid lines in Figure 1). We attribute the small drop in count rate below 1.4 to a too-small source model of 100 cm radius. Low formation density results in less absorption of radiation, so the detector might ‘see’ outside the 100 cm; in other words, the simulated source in this case is not an infinite

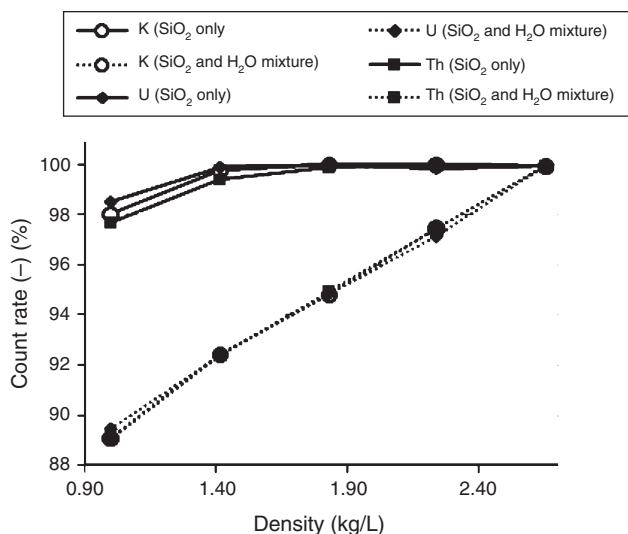


**Fig. 1.** Count rate as a function of density for K, U and Th in both a pure  $\text{SiO}_2$  and a  $\text{SiO}_2$ /water mixture matrix. Count rates are normalised to the situation with 2.65 kg/L density (i.e. 100%  $\text{SiO}_2$ ). The water fraction  $f$  per plotted density can be calculated from  $\rho = f + (1 - f) \times 2.65$  or  $f = (2.65 - \rho)/1.65$ .

one. Since Maučec et al. (2009) used only a 50 cm radius model as ‘infinite’ source in their simulations, their results deviate even more than ours. Their conclusion of density affecting count rate is therefore incorrect.

The second set of Monte Carlo simulations with changing density assumes the pore space in the  $\text{SiO}_2$  matrix to be filled with water. The result is not only a change in density, but also in composition of the formation. Most notable is an increase in the average number of electrons per nucleon due to the introduction of hydrogen. As a result, the cross-section for photon attenuation will increase when the formation density decreases (Storm and Israel, 1970), which leads to a higher probability for gamma radiation to be absorbed. This effect is visible in Figure 1 as the dotted lines. For all three radio nuclides, the drop in count rate is more than 10% when the formation is changed from 1 kg/L  $\text{SiO}_2$  to pure water.

### Effects of borehole diameter

To estimate the effects of the borehole diameter on the count rate of a borehole probe, we created a set of Monte Carlo models with, again, a  $50 \times 150$  mm BGO crystal placed in the centre of boreholes with various diameters. The borehole is empty, so no absorption occurs inside the borehole, and effects, if any, are solely coming from the change in geometry. The formation is basically infinite, but was limited in the models to a 400 cm long cylinder with an 80 cm radius.

Similar to Maučec et al. (2009), we find only a slight decrease in count rate as the borehole diameter increases (Figure 2); however, this occurs to a much lesser extent than Maučec et al. (2009), who find a drop in the count rate of around 30% for a borehole diameter of 40 cm. We attribute the observed decrease in count rate, again, to be a result of the Monte Carlo model of Maučec et al. (2009) not fully representing an infinite formation.

Apparently borehole diameter does not affect the count rate. This implies the flux of gamma radiation inside the borehole is not affected by the borehole size. This can be understood as follows:

- For an infinite, perfectly homogeneous formation (without a borehole), gamma-ray production and absorption is in equilibrium everywhere, and the flux of gamma radiation is constant over the complete volume.
- Assuming we drilled an empty (vacuum) borehole inside our endless volume, this void will not absorb any radiation; therefore, the flux at any point *inside* our borehole will be identical to that on the wall of the borehole.
- At each point on the wall, the flux exiting the formation into the borehole is therefore equal to the flux going from the borehole into the formation.

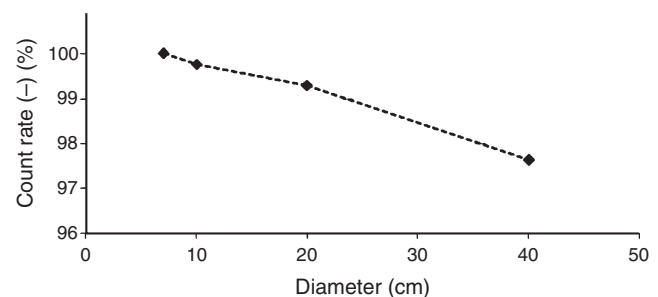


**Fig. 2.** Count rate in the  $^{232}\text{Th}$  spectrum above 300 keV as a function of borehole diameter in an empty borehole. Count rates are normalised to the count rate for a borehole diameter of 7 cm.

- In other words, flux is not affected by the borehole, which is in agreement with our observation of the borehole diameter not affecting count rate.

### Attenuation by borehole fluid

Although we have shown that the diameter of an empty (vacuum) borehole has no effect on count rate, filling it with fluid will presumably cause count rate to drop.

In order to estimate the magnitude of the absorption, we ran a large series of Monte Carlo simulations for varying fluid density, borehole diameter and probe diameter. Schlumberger (2009) combined these parameters into a variable  $t$ :

$$t = W \times \frac{d_h - d_t}{2}, \quad (1)$$

where  $W$  is the density of the borehole fluid in  $\text{g/cm}^3$ , and  $d_h$  and  $d_t$  are the borehole and probe diameters in cm.

Schlumberger (2009) presents charts with correction curves for probes with two different diameters: both for the probe centred in the borehole and for the probe positioned against the wall.

For the Monte Carlo simulations, we made models with six different values of  $d_t$  (up to 3.4 inch diameter), seven values of  $d_h$  (up to 12 inch) and four values of  $W$ . Each possible combination, where the  $d_t \leq d_h$ , was run six times for each nuclide  $^{40}\text{K}$ ,  $^{238}\text{U}$  and  $^{232}\text{Th}$  with the probe both centred and against the wall. The borehole fluid modelled is either air ( $W = 1.29 \times 10^{-3} \text{ g/cm}^3$ ) or a water/bentonite mixture, where bentonite was modelled as pure  $\text{SiO}_2$  with a matrix density of  $2.65 \text{ g/cm}^3$ . With water modelled as  $\text{H}_2\text{O}$  with  $1.00 \text{ g/cm}^3$  density, the resulting mixture has values of  $W$  ranging from 1.0 (pure water) to  $1.4 \text{ g/cm}^3$ .

The modelled detector is a simple NaI crystal with variable diameter and a length of 4 inch. The modelled volume is restricted by an ellipsoid of  $120 \times 120 \times 180 \text{ cm}$ . Surrounding this ellipsoid is another ellipsoid of  $140 \times 140 \times 210 \text{ cm}$  (see Figure 3), which has the same material properties, but is not a source of gamma particles. The longest axis of the ellipsoids is also the centre of the borehole.

The result of each simulation is a spectrum which the detector would collect for a  $1 \text{ Bq/kg}$  activity in the formation. From this spectrum the count rate was taken between 0.3 and 3.0 MeV. As expected, the count rate decreases for increasing values of  $t$ . Similar to the approach by Schlumberger (2009),

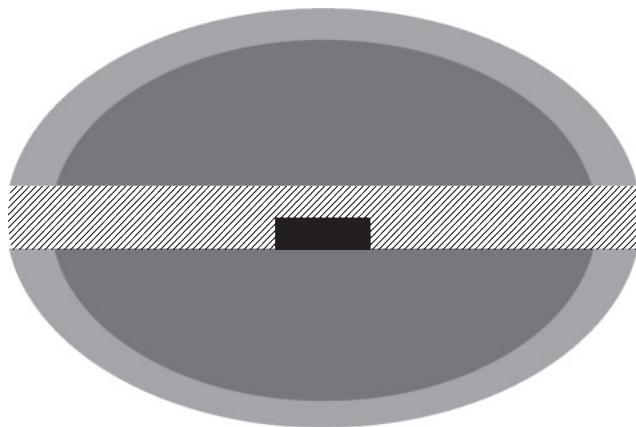


**Fig. 3.** Cross-section of the Monte Carlo model (not to scale) with the detector (black) against the wall of the borehole (hatched). The formation (grey) is only partially modelled as a source of gamma radiation (dark grey).

we have determined a correction factor  $F$  for each situation, which is defined as the count rate in the  $t = 0$  situation divided by the count rate in the specific situation. Figure 4 shows  $F$  as a function of  $t$  for different probe diameters. The dotted lines show a least-squares best fit according to the equation:

$$F = (c_0 + c_1 d_t t) \times e^{c_2 t}. \quad (2)$$

From Figure 4, it is obvious that larger probe diameters require larger correction values for increasing values of  $t$ , but it should be noted that a larger probe inside a specific borehole yields a smaller value of  $t$  (Equation 1). For the two probe diameters in the correction charts by Schlumberger (2009), the largest probe diameter also has the largest correction factor  $F$ .

Moving the detector to the side of the borehole will obviously lower the absorption of the fluid, as seen in Figure 5. This figure plots the required correction factor  $F$  as a function of  $t$  for different probe diameters for the off-axis situation. As expected, larger values of  $t$  require larger correction values, but  $F$  is smaller than in the ‘axial’ case.

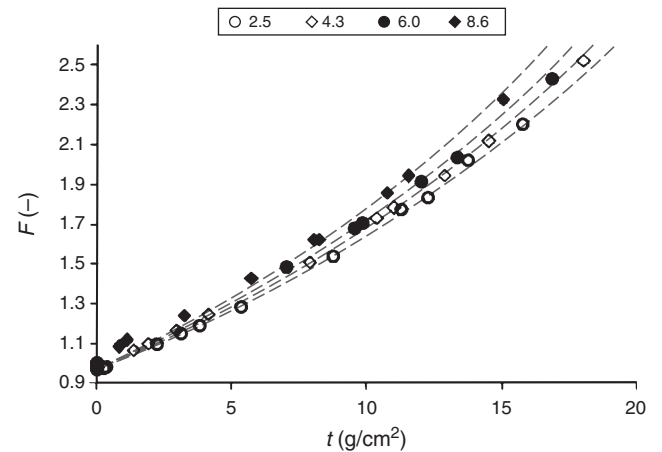


**Fig. 4.** Correction values  $F$  required to convert the observed count rate back to the count rate at  $t = 0$  (i.e. a borehole without fluid) for count rates in the 0.3 to 3.0 MeV energy range of the  $^{238}\text{U}$  spectrum when the probe is centred in the borehole. Data for probe diameters 2.5, 4.3, 6.0 and 8.6 cm. Dotted lines indicate the best fit.

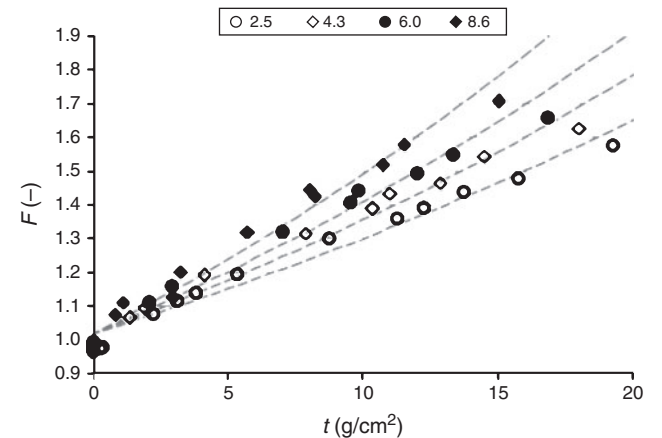


**Fig. 5.** Correction values  $F$  required to convert the observed count rate back to the count rate at  $t = 0$  (i.e. a vacuum filled borehole) for count rates in the 0.3 to 3.0 MeV energy range of the  $^{238}\text{U}$  spectrum when the probe is located against the wall of the borehole. Data for probe diameters 2.5, 4.3, 6.0 and 8.6 cm. Dotted lines indicate a best fit.

As before, a combination of probe diameter  $d_t$  and  $t$  appear to be good proxies to describe the correction factor, but the correlation is less accurate. Nevertheless, a best fit following Equation 2 still yields a good approximation of the correction values found using MCNP.

The Monte Carlo simulations returned full spectrum data. This allows us to check whether the corrections  $F$  we just modelled are good enough to properly compare spectra taken at different borehole environments. Figure 6 illustrates the strength of the method by overlaying two  $^{232}\text{Th}$  spectra taken in completely different boreholes. After compensation, there is hardly any observable difference between the spectra.

### Attenuation by casing

Steel or PVC casing between the formation and the borehole will absorb some of the radiation, causing a reduction of the detector count rate. We ran a set of Monte Carlo models to estimate the effect of casing thickness on the collected count rate. As before, the count rate is determined from spectra in the 0.3 to 3.0 MeV range.

In our simulations, the steel casing was modelled as having a fixed thickness of 0.1 mm and a ‘fictional’ density ranging from 80 to 640 kg/L, corresponding to steel casings with density 8 kg/L and ranging in thickness from 1 to 8 mm. Using this approach, we made sure any effects on the collected spectrum are caused by absorption in the casing, and not by a change in the geometry. Figure 7 shows the relative count rate as a function of the apparent casing thickness.

The absorption effect of a steel casing and borehole fluid are comparable since both can geometrically be regarded as a hollow cylinder of absorbing material between the formation and the detector. The equations determined to correct for the absorption by borehole fluid can be applied to correct for the steel casing as well. The variable  $t$  in Equation 2 can now be determined as:

$$t = W \times d_c, \quad (3)$$

where  $W$  is the density of the casing in kg/L and  $d_c$  is the thickness of the casing in cm.

When applying the correction equations with the parameters  $c_i$  as determined before, the result is remarkably good, as shown in Figure 6. For all three radio nuclides, and for all modelled casing thicknesses, the corrected count rate is within

2% of the count rate found for the simulation where no casing is modelled.

### Calibration pits compared

Back in the early 80s, studies were already performed to cross-calibrate several testing pits around the world (for example see Bristow et al., 1982). However, there seems to be only limited data available that interlinks these pits for spectral gamma tool calibrations, and comparisons that were made mainly focussed on the uranium pits (Dickson, 2012). In this section, we present some data taken at pits in Grand Junction and Adelaide and compare it to the measurements we did at our ‘home’ calibration setup in The Netherlands (Stonehenge). We have calibrated many borehole probes using the Medusa Stonehenge calibration set-up (van der Graaf et al., 2011), with several probes having a  $1 \times 4$  inch BGO detector. A few of these were also sent to the calibration facilities in Grand Junction, USA (US Department of Energy, 2013) and the Adelaide AM-6 calibration pits in Adelaide, Australia (Dickson, 2012).

In short, the procedure we developed for creating standard spectra comprises the following steps:

- 1) A detailed source-detector model is made for the probe inside the Medusa Stonehenge set-up. This model comprises a detailed sketch of the probe and source, as well as information on the composition of the different parts (material types, densities and shape).
- 2) Using the MCNP (Waters et al., 2007) simulation code, the response of the detector inside the source is obtained. The result of the simulation is a histogram record, i.e. the spectrum one would expect for this detector inside the calibration setup.
- 3) Afterwards, a measurement is made with the actual probe inside the calibration source. Using this data, the histograms are Gaussian broadened and corrected for efficiency, offset and non-linearity of the probe.
- 4) The result is a set of ‘standard spectra’, i.e. the response of the detector for a source of 1 Bq/kg of  $^{40}\text{K}$ ,  $^{238}\text{U}$  or  $^{232}\text{Th}$ .

The Stonehenge calibration facility is a brick castle (height 100 cm, width 120 cm, depth 100 cm) with an 80 cm deep opening at the front in which a detector can be placed for

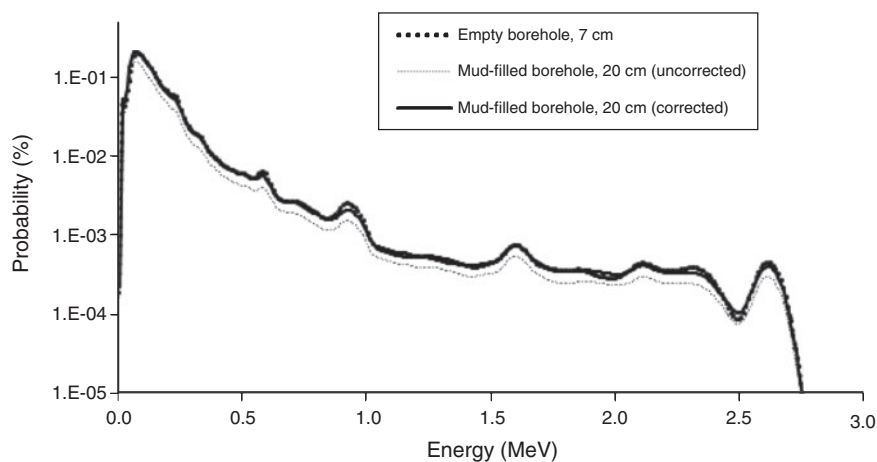


**Fig. 6.**  $^{232}\text{Th}$  spectra from simulations for a 1 inch diameter probe positioned against the wall of the borehole. One spectrum is for an empty (vacuum) borehole of 7 cm diameter, which does not need correction ( $F=1$ ). The other spectra are for the same probe, but in a 20 cm diameter borehole filled with bentonite mud with a density of 1.4 kg/L. After correction ( $F=1.43$ ), this spectrum is almost identical to the spectrum for the empty borehole.

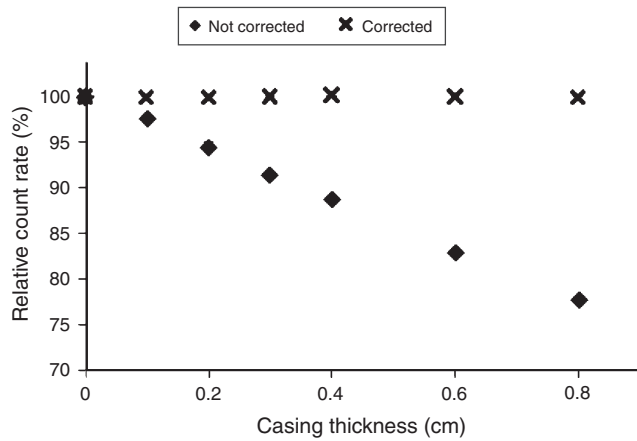


Fig. 7. Count rate in the  $^{40}\text{K}$  spectrum as a function of casing thickness before correction (squares) and after correction (crosses). The count rate is relative to the count rate observed when no casing is present.

testing. The bricks are normal-sized ( $10 \times 20 \times 6.5 \text{ cm}^3$ ) Dutch paving bricks that consist of baked clay and were purchased in one batch to minimise inter-brick variations. The density of the bricks is  $2320 \text{ kg/m}^3$ . Ideally, a calibration facility should be infinitely large enough that all radiation that contributes to the count rate of the detector surface originates from the facility. van der Graaf et al. (2011) showed that the Stonehenge facility is very similar to an infinite geometry. Influences of the floor and wall of the storage hall in which the facility is situated are estimated to contribute less than 0.1% to the signal in the detector being tested, and this amount of radiation is suspected to be from the bricks in the Stonehenge facility itself. As a consequence no extra shielding (e.g. with lead or copper) of the facility is needed.

The Stonehenge clay bricks only contain the natural activity that is incorporated in the clay from which they were manufactured. The activity concentrations of K, U and Th were measured on crushed samples (grain size of less than 3 mm) from one of the Stonehenge bricks. Furthermore, to assess the variation between the bricks of Stonehenge, 10 bricks were cleaved in two geometrically identical halves. Each half brick was individually measured for at least 1 h (resulting in the uncertainties from counting statistics to be smaller than 1%). For all three radionuclides, the homogeneity of the activity concentration, defined as the ratio of the standard deviation versus the mean of the 20 half bricks, is better than 3.5%. For the analysis in this study, we compared all measurements to the Stonehenge calibration facility.

The concentrations listed for the Stonehenge facility (1.64%  $^{40}\text{K}$ , 3.0 ppm eU and 11.7 ppm eTh) are relatively low, especially in eU and eTh. One can argue that these concentrations are not representative for the measurements in the Adelaide and Grand Junction models. However, a spectral gamma tool having proper dead-time and pileup correction should not show any efficiency deviations for the source strengths listed here. We therefore assume a comparison is possible.

The spectra recorded by the probes in Grand Junction and Adelaide have been analysed using the full spectrum analysis software GAMMAN (Hendriks et al., 2001), with the standard spectra obtained as a result of the Stonehenge calibration.

Using the correction algorithms described before, we corrected the Adelaide and Grand Junction datasets for their respective borehole properties. That way, we arrive at absolute activity concentrations for these calibration pits. The results of these measurements are shown in Tables 1 and 2, along with the known 'listed' activity concentrations.

Table 1. Activity concentrations in % or ppm for three Grand Junction pits (known as the K, U and Th models).

Listed concentrations from US Department of Energy (2013).

Pit	Listed	Before correction	After correction
$^{40}\text{K}$	5.34%	4.14%	5.14%
$^{238}\text{U}$	421 ppm	321 ppm	441 ppm
$^{232}\text{Th}$	413 ppm	316 ppm	422 ppm

Table 2. Activity concentrations in % or ppm for three zones in the Adelaide AM-6.

Data taken from <http://members.optusnet.com.au/~drpl/Pit%20AM06.html>.

Zone	Listed	Before correction	After correction
$^{40}\text{K}$	4.3%	3.70%	4.04%
$^{238}\text{U}$	34.1 ppm	28.3 ppm	32.9 ppm
$^{232}\text{Th}$	62.7 ppm	50.2 ppm	57.6 ppm

From the activity concentrations in Tables 1 and 2, it is apparent that uncorrected measurements do not correspond at all to the listed values. But as one expects, following the correction, the activity concentrations correspond much better:  $^{40}\text{K}$  is 4% and 11% lower,  $^{238}\text{U}$  is 5% and 3% higher and  $^{232}\text{Th}$  is 2% higher and 5% lower compared to the pits of Grand Junction and Adelaide, respectively.

The differences between listed and corrected values are relatively small and can be attributed to uncertainties both in the listed pit grades and in the gamma-ray data used. Obviously one can expect that the correlation found between the three calibration pits will improve by using data from other tools with differing crystal sizes and types. At the same time, we think our results are promising because they show that data taken in calibration set-ups with strongly differing geometry and composition can indeed be compared. This opens the way towards a global network of interconnected calibration facilities as was envisaged by Bristow et al. (1982).

## Conclusions

Our full spectrum MCNP simulations clearly confirm the well known fact that borehole diameter, probe diameter, borehole fluid and casing thickness significantly affect the intensity of the gamma spectrum. An important finding, however, is that the *shape* of the spectrum is hardly influenced at all. In other words, for all practical purposes, the compensation of energies between 0.3 and 3 MeV can be considered equal. This greatly simplifies the compensation algorithms to energy-independent scaling laws.

Formation density and the diameter of an empty (vacuum) borehole do not significantly affect the spectra. However, the presence of water or heavier borehole fluid does reduce the spectral intensity, a reduction that can be compensated for by using a relatively simple formula that has thickness and density of the absorbing layer and detector diameter as parameters. A similar approach allows us to also compensate borehole data for casing thickness and make.

The application of the scaling laws found to date at facilities in Grand Junction and Adelaide are very promising. We show that by using calibration data taken at a completely different set-up (the Stonehenge facility in The Netherlands), we can correctly reconstruct the K, U and Th grades of the pits in the US and Australia. Of course, more tests with different tool types are needed, but the promise of having a proper, simple and uniform set of scaling laws that interconnect several

calibration stations around the world motivates further study. After all, not having to ship tools around the world for calibration greatly simplifies life for the wireline loggers!

### Acknowledgements

The authors wish to thank Annick Henriette, Patrick van Eyll (ALT), John Stowell (Mt Sopris), Duncan Cogswell (Borehole Wireline) and Paul Worthington (Robertson Geologging) for sharing data and commenting on our research.

### References

- Bristow, Q., Killeen, P. G., and Mwenifumbo, J. C., 1982, Comparison of standardized gamma-ray log calibration measurements: Ottawa, Adelaide and Grand Junction: *Proceedings of the Symposium on Uranium Exploration Methods*, 715–726.
- Dickson, B., 2012, Reassessment of the grades of the Adelaide model logging pits: *Preview*, **2012**, 20. doi:10.1071/PVv2012n159p20
- Dickson, B., and Beckitt, G., 2013, The application of Monte Carlo modelling to downhole total-count logging of uranium: part I – low grade mineralisation: *Exploration Geophysics*, **44**, 56–62. doi:10.1071/EG12018
- Hendriks, P. H., Limburg, J., and de Meijer, R. J., 2001, Full-spectrum analysis of natural gamma-ray spectra: *Journal of Environmental Radioactivity*, **53**, 365–380. doi:10.1016/S0265-931X(00)00142-9
- Maučec, M., Hendriks, P. H. G. M., Limburg, J., and de Meijer, R. J., 2009, Determination of correction factors for borehole natural gamma-ray measurements by Monte Carlo simulations: *Nuclear Instruments and Methods in Physics Research Section A: Accelerators, Spectrometers, Detectors and Associated Equipment*, **609**, 194–204. doi:10.1016/j.nima.2009.08.054
- Schlumberger, 2009, *Log interpretation charts*: Schlumberger.
- Storm, L., and Israel, H. L., 1970, Photon cross sections from 1 keV to 100 MeV for elements Z=1 to Z=100: *Atomic Data and Nuclear Data Tables*, **7**, 565–681. doi:10.1016/S0092-640X(70)80017-1
- Stromswold, D. C., 1995, Calibration facilities for borehole and surface environmental radiation measurements: *Journal of Radioanalytical and Nuclear Chemistry*, **194**, 393–401. doi:10.1007/BF02038439
- US Department of Energy, 2013, *Field calibration facilities for environmental measurement of radium, thorium, and potassium* (S07707/4 edition): US Department of Energy.
- van der Graaf, E. R., Limburg, J., Koomans, R. L., and Tijs, M., 2011, Monte Carlo based calibration of scintillation detectors for laboratory and in situ gamma ray measurements: *Journal of Environmental Radioactivity*, **102**, 270–282. doi:10.1016/j.jenvrad.2010.12.001
- Waters, L. S., McKinney, G. W., Durkee, J. W., Fensin, M. L., Hendricks, J. S., James, M. R., Johns, R. C., and Pelowitz, D. B., 2007, The MCNPX Monte Carlo radiation transport code: *AIP Conference Proceedings*, **896**, 81–90.
- Weatherford, 2006, *Wireline services log interpretation chart book* (2006 edition): Weatherford Inc.